Effects of High Water Vapor Pressures on the Oxidation of SiC-Based Fiber-Reinforced Composites

K.L. More, P. F. Tortorelli, and L.R. Walker
Oak Ridge National Laboratory
Metals and Ceramics Division
Oak Ridge, TN, USA 37831-6064

Keywords: ceramics, composites, microstructures, water vapor, boron nitride, silicon carbide

ABSTRACT

The oxidation of SiC-fiber-reinforced SiC composites at high temperature (1200°C) and elevated total water vapor pressures (up to 1.5 atm) was studied. Substantial degradation of SiC composites was observed under these exposure conditions, particularly when BN (used as a fiber coating) was a composite constituent. Besides accelerated SiC recession due to oxidation, the reactions of oxygen and H_2O with boron and between boria and SiO_2 led to extensive borosilicate glass formation as well as some volatile $H_xB_yO_z$ products. The extent of these reactions and the rate of overall degradation were compared for different as-processed structures by exposing composites fabricated by processes such as chemical-vapor- and silicon melt-infiltration. Microstructural and compositional factors such as the amount of interconnected porosity and total boron content in the composite had important influences on the rate of degradation. Based on the present results, the overall oxidation behavior of the different composites at high water vapor pressures can be explained based on the concurrent surface reactions involving the formation of volatile reaction products, borosilicate glass, and silica.

1. INTRODUCTION

Significant advances in SiC-based continuous fiber-reinforced ceramic matrix composite (CFCC) development and design have been made over the past few years and have led to the implementation of these materials in several high-temperature applications. Improvements in ceramic fiber stability and composition, interfacial coatings, and matrix chemistry and densification have resulted in composites with superior mechanical properties and enhanced resistance to oxidation. While the fiber reinforcement and matrix are critical for the strength and environmental stability of a composite, it is the fiber-matrix interface that ultimately controls the composite fracture behavior and the retention of such at elevated temperatures in corrosive environments. Chemical vapor deposited (CVD) boron nitride is currently the preferred interfacial component utilized by CFCC manufacturers. At room temperature, BN fiber coatings allow for the fiber-matrix debonding characteristic of tough composites.[1,2] However, in oxygen- and especially water-containing environments, BN undergoes rapid degradation that can negatively impact the usefulness of the composite in the long term.[3-6]

The deleterious effect of water vapor (0.1-0.9 atm) on SiO_2 growth on Si-based ceramics is well documented.[7-9] More recently, work has been conducted at higher water vapor pressures (>1 atm)

typical of those in many gas turbines.[10,11] Based on these results and since most SiC-based composites are composed of SiC materials (SiC fibers and matrix) comprising >90 vol% of the system, accelerated oxidation of the composite in high H_2O environments should be very similar to that observed for monolithic SiC. However, as shown below, this is not necessarily the case. The issue of understanding *composite* degradation has become an extremely important one since several differently processed SiC fiber-reinforced SiC matrix CFCC combustor components in land-based gas turbines are currently being evaluated in actual engine tests.[11,12] All of these commercial composites contain BN interfacial coatings. As a result, it has become imperative to fully understand the degradation mechanisms associated with the use of SiC/BN/SiC materials in high water-vapor-containing environments and to develop an understanding of the primary issues associated with the long-term stability of several different SiC/BN/SiC composites.

To this end, recent work has focused on the evaluation of several commercially available SiC/BN/SiC composites exposed to high water-vapor pressures in a high-temperature, high-pressure laboratory-scale exposure facility. In particular, oxidation mechanisms for the various CFCCs were evaluated based on the particular composite processing method and starting composition. Of primary importance was the contribution of BN and B-containing compounds to the overall rate of composite degradation in these oxidizing environments.

2. EXPERIMENTAL PROCEDURE

Two different commercial SiC/BN/SiC composites were used in this study. The first was a composite with continuous Hi-Nicalon™ SiC fiber reinforcement, CVD BN interfacial coatings, and a SiC matrix processed using the isothermal chemical vapor infiltration (CVI) technique at Honeywell Advanced Composites, Inc.[13] The second type of SiC/BN/SiC material, which is manufactured by both B.F. Goodrich Aerospace and Honeywell Advanced Composites, Inc., also contained Hi-Nicalon™ fibers and CVD BN interfacial coatings, but had a SiC matrix fabricated using the silicon melt-infiltration (MI) process.[14] Both of these manufacturing techniques have been used to make full-scale CFCC combustor liners (33 cm diameter inner liner and 76 cm diameter outer liner) for engine tests.[12]

As-processed coupons of each type of CFCC were exposed in a high-temperature, high-pressure exposure facility, which has been described in detail elsewhere.[15] In order to simulate the water vapor pressure of the combustor environment, all tests were conducted at ~1200°C, 10 atm total pressure, and 1.5 atm H_2O. Each exposure was 500 h, after which time the specimens were carefully removed and selectively cut for microstructural analysis. Specimens were then placed back in the furnace for additional exposure time. The CFCCs used in this work were exposed for up to 3000 h.

Microstructural examinations were conducted after each 500 h exposure to measure both oxide product thickness and surface recession and to assess the oxidation-induced structural damage to the different CFCCs and their constituents. Electron probe microanalysis (EPMA) and backscatter electron imaging (BSE) were the primary analysis techniques used to examine CFCC cross-sections before and after exposure. Transmission electron microscopy (TEM) was also conducted on selected specimens, but these results are not presented here.

3. RESULTS

3.1 As-Processed CFCC Microstructures

The two SiC/BN/SiC composites compared in this study have different starting microstructures. The CVI composites are characterized by a 2-D woven fiber structure with a 0°/45° fiber lay-up, as shown in the relatively low magnification BSE image in Figure 1a. In addition to the CVD BN interfacial coating, a B-containing particulate "filler" is used within the fiber tows. The fiber-coating structure within the fiber tows for the CVI composite is shown in Figure 1b. The BN-coated fibrous preform was then densified with SiC by CVI. The resulting CVI composite is ~85-95% dense.

A similar fiber lay-up was used for the MI SiC/BN/SiC composite, as shown in Figure 2a. The MI SiC/BN/SiC utilizes a uniformly thin, continuous CVD BN coating, ~0.4 μm thick, around the fibers. To protect the BN- coated fibrous preform during MI processing, a thin (~1-2 μm) CVI SiC layer was applied around the tows (see Figure 2b). This minimal CVI step leaves a fairly open structure for subsequent molten silicon MI processing while still protecting the fibers and fiber coatings. After processing, the MI matrix is primarily Si+SiC and the composite is near full density. Composite density differences are clearly evident in the images shown in Figure 3, which compares the bulk microstructure of the CVI and MI SiC/BN/SiC composites. Large, interconnected matrix porosity is characteristic of most CVI composites, whereas MI composites are much denser.

3.2 Analysis of Exposed MI SiC/BN/SiC

The MI composite was exposed to 1.5 atm H_2O at 1200°C for a total of 3000 h. During this time, extensive microstructural damage occurred. Figure 4 shows images of the bulk composite recession (measured as loss of useful composite) and concurrent silica scale formation on the MI SiC/BN/SiC surface as a function of exposure time. The surface of the MI SiC/BN/SiC before oxidation was composed primarily of the Si+SiC MI matrix, whether thinly covering a fiber tow or as large scale matrix between tows, as shown in Figure 5. The composite can be considered as a complex layered structure of the different constituents (see Figure 5) which are oxidized in sequence as the oxidation front progresses through the structure. Thus, the MI matrix (Si+SiC) oxidizes first followed by the CVI SiC layer around the fiber tows. Each constituent oxidizes at a different rate, consuming one layer and then moving through the next while producing different reaction products with very different product morphologies. Once the CVI SiC layer around the fibers is breached, oxidation of the fiber tows is very rapid, faster than the surrounding constituents, and occurs primarily via the rapid oxidation along/through the BN interfaces, as shown in Figure 6a. The BN acts as a conduit for rapid transport of oxidant within the fiber tow and clearly oxidizes much faster than the surrounding SiC and SiC fibers. Within the tows, the fibers are completely consumed after they become surrounded by the oxidized BN. The oxidation damage around individual fibers within a tow is shown clearly in Figure 6. A fully consumed fiber tow serves as the path for the progression of the oxidation front further into the composite (see Figure 6b). Areas that are primarily MI Si+SiC matrix will oxidize rapidly,[10] but not as rapidly as the fiber tows since the tows contain the thin, but continuous, BN.

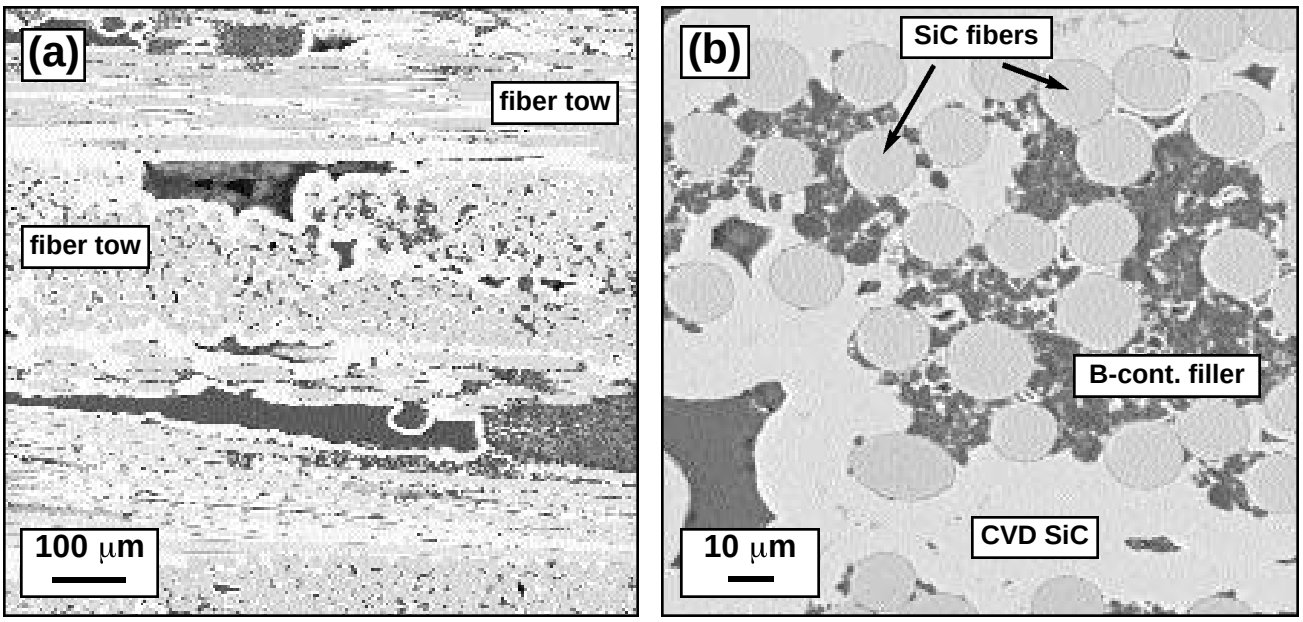

Figure 1. Microstructure of as-processed CVI SiC/BN/SiC composite (a) bulk fiber-matrix structure and (b) structure within fiber tows. Arrows in (b) show B-containing filler component.

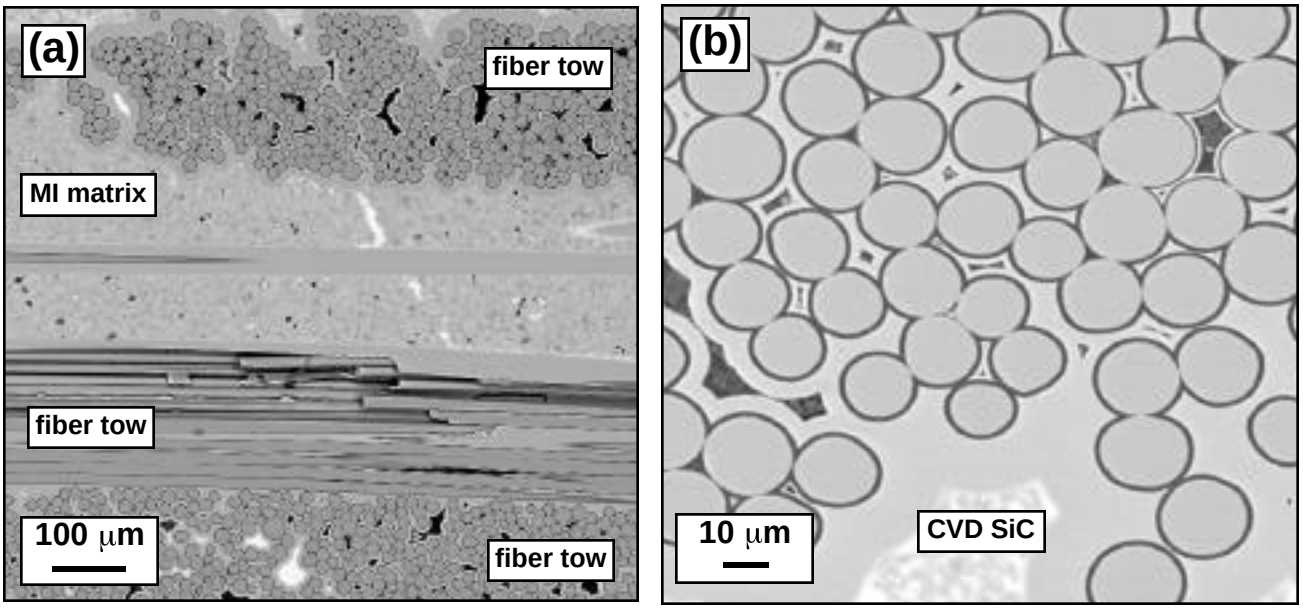

Figure 2. Microstructure of as-processed MI SiC/BN/SiC composite (a) bulk fiber-matrix structure and (b) structure within fiber tows. Note uniformity of thin ~0.4 μm BN interface around fibers.

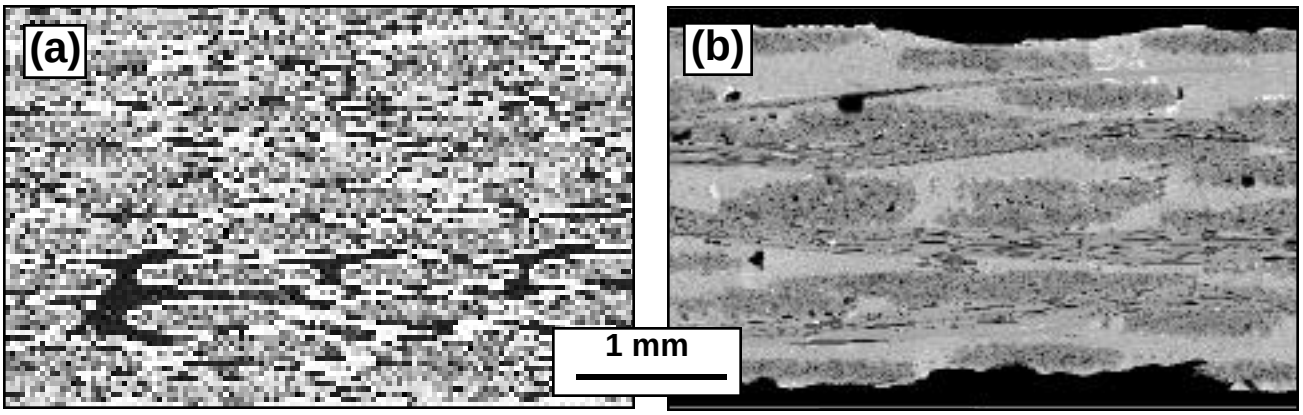

Figure 3. Composite density differences between (a) CVI and (b) MI SiC/BN/SiC composites. Also compare Figure 1a and Figure 2a.

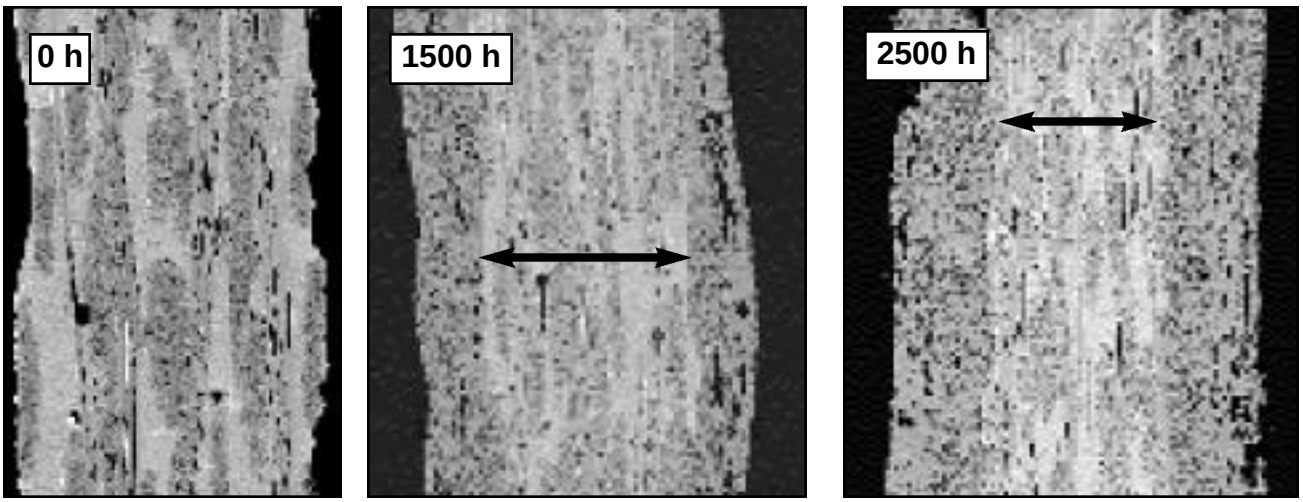

Figure 4. Surface recession and scale formation on MI SiC/BN/SiC composite after exposure for different times at 1200°C and 1.5 atm H_2O.

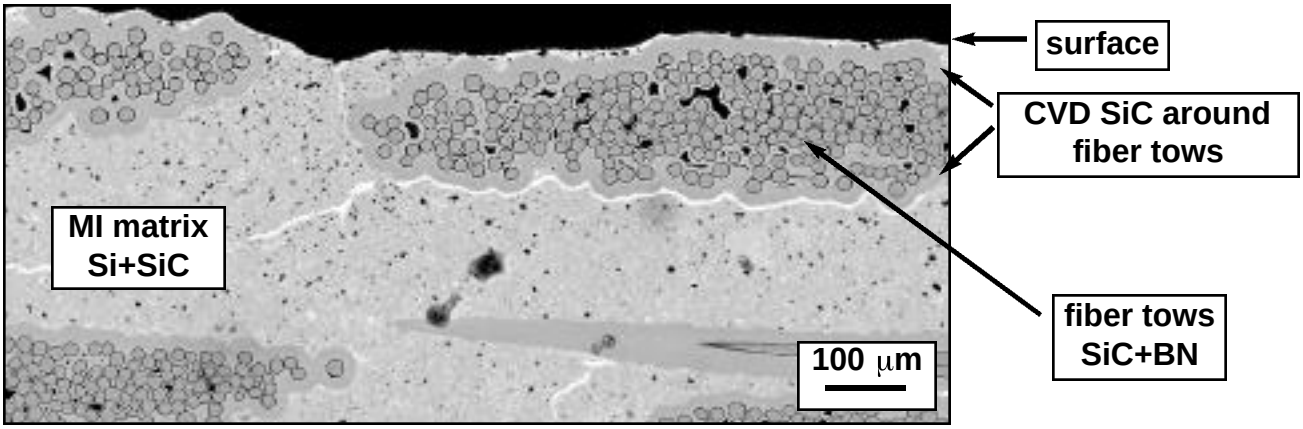

Figure 5. Surface of as-processed MI SiC/BN/SiC showing all composite constituents.

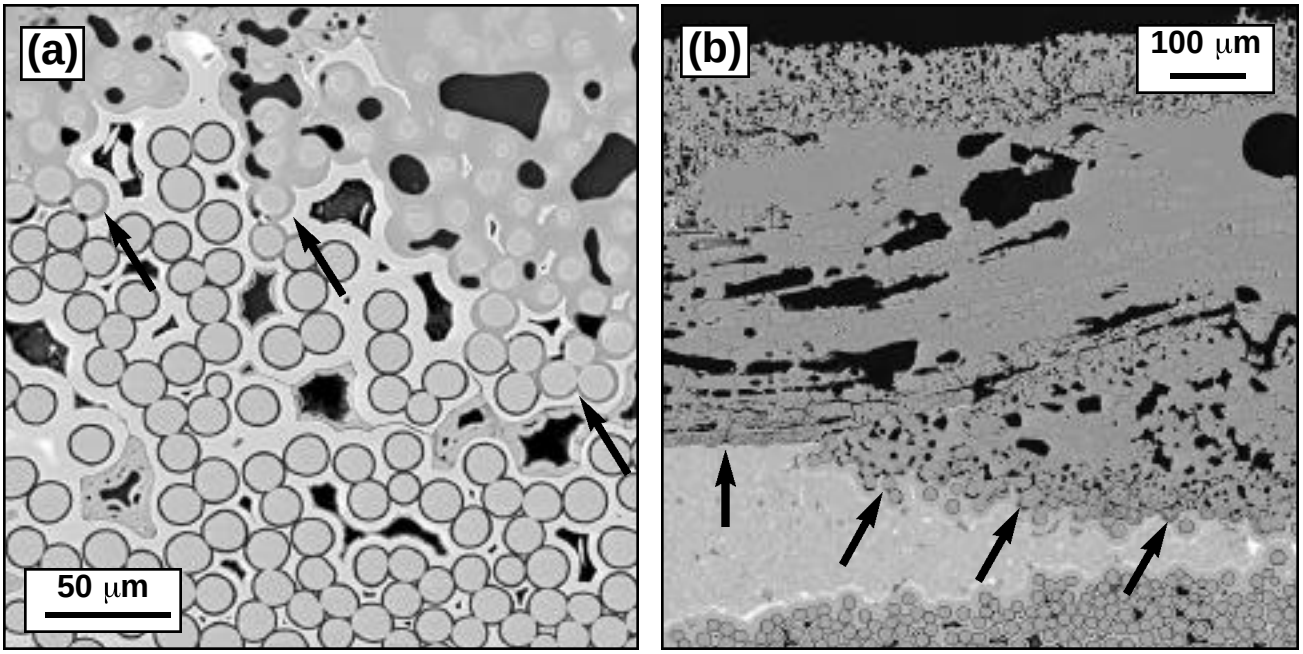

Figure 6. BSE images showing (a) oxidized BN interfaces within a fiber tow and (b) accelerated damage within the fiber tow compared to the matrix in MI SiC/BN/SiC.

3.3 Analysis of Exposed CVI SiC/BN/SiC

The CVI composite was only exposed for 1500 h at 1200°C and 1.5 atm H_2O before extensive composite damage prevented reintroduction into the exposure facility. Figure 7 is an image of the coupon cross-section after 1500 h at 1200°C. Note the very thick, highly voided scale on the surface of the CVI SiC/BN/SiC which had a much different morphology than that observed on the MI composite (see Figure 4). Fiber tows near the exposed surface were oxidized in a similar manner to that observed for the MI SiC/BN/SiC, albeit more severely and rapidly, as shown in Figure 8 (compare to Figure 6) as a result of substantial borosilicate glass formation in these areas. In addition to the extensive surface oxidation, sub-surface oxidation within the large, interconnected porosity was observed in the CVI SiC/BN/SiC. During the first 500 h exposure, thin silica scales formed on the CVI SiC matrix surrounding the sub-surface porosity, as shown in Figure 9a. With additional exposure, the CVI SiC matrix around the porosity below the surface was breached. Rapid degradation of the B-containing filler material and the CVD BN fiber coatings within the tows then occurred, as shown in Figure 9b. Entire sub-surface fiber tows were consumed by this process and pools of glass were formed in these areas well below the exposed surface. Thus, for the CVI SiC/BN/SiC, oxidation was not simply limited to the exposed surface of the composite. Rapid degradation in this case was compounded by sub-surface accumulation of oxidation-induced damage.

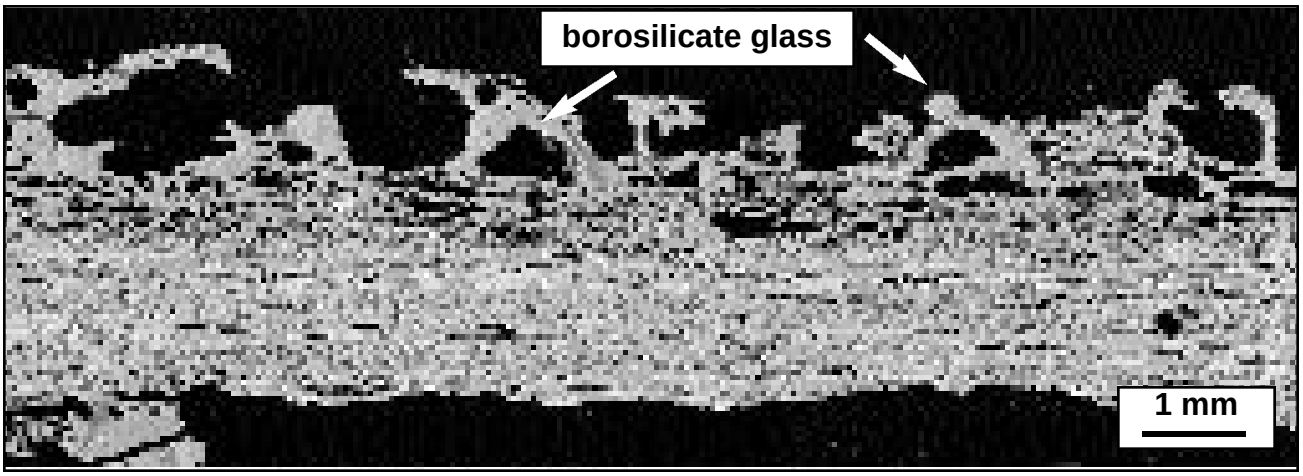

Figure 7. Low magnification BSE image of a CVI SiC/BN/SiC composite cross-section showing excessive glass formation at specimen surface after 1500 h at 1200°C and 1.5 atm H_2O.

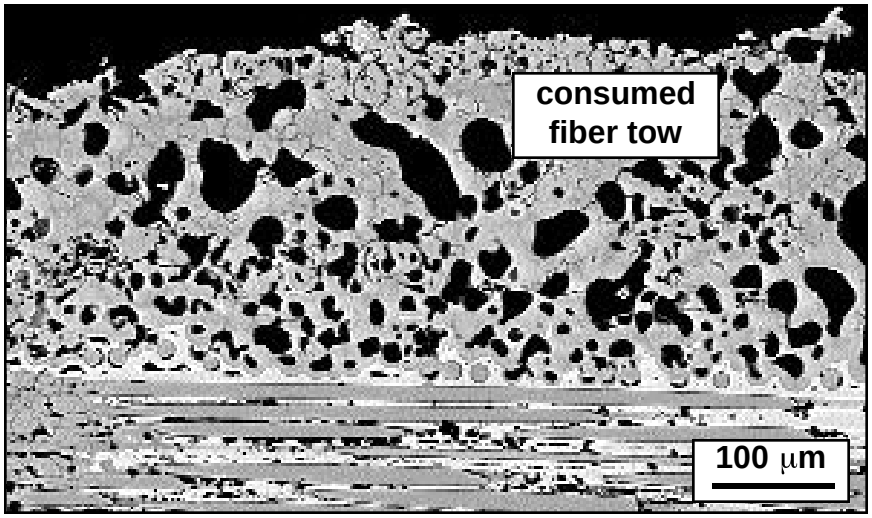

Figure 8. Damage within a near-surface fiber tow in CVI SiC/BN/SiC composite after 1500 h at 1200°C and 1.5 atm H_2O.

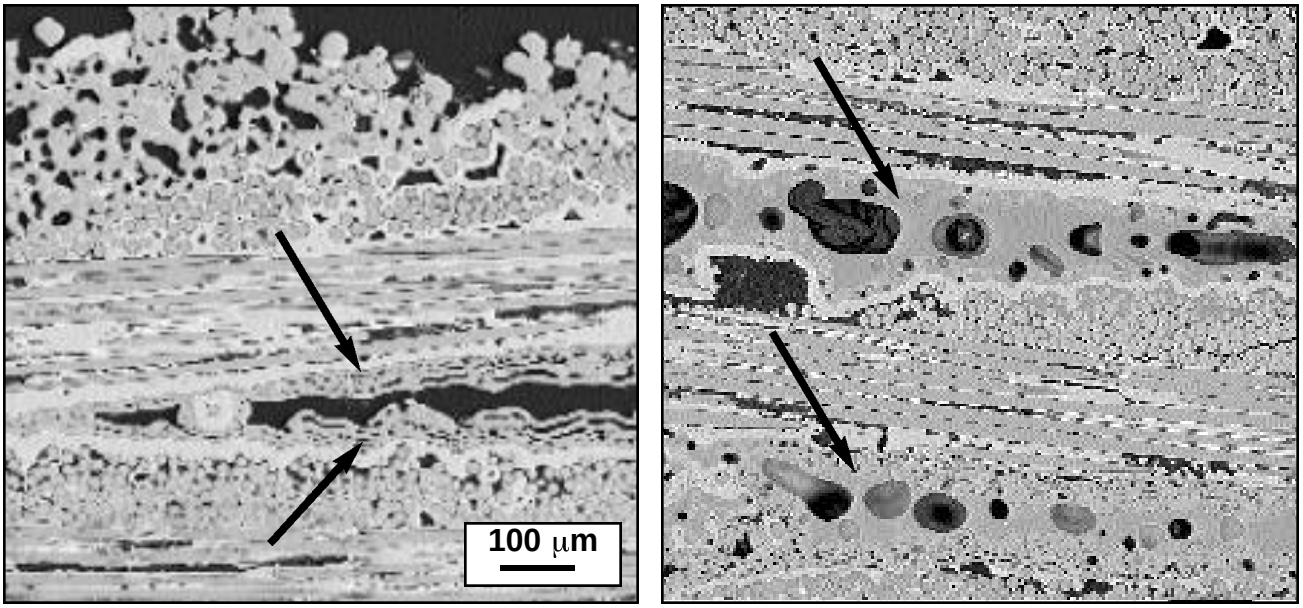

Figure 9. BSE images showing oxidation of CVI SiC matrix within (a) a sub-surface pore after 500 h and (b) a sub-surface pore after 1500 h where the SiC has been breached and excessive oxidation-induced damage is evident below the exposed surface.

4. DISCUSSION

The rates for composite oxidation were much higher than that measured for pure CVD SiC at 1200°C and 1.5 atm H_2O, as shown in Figure 10.[10] Also, the rate of CVI SiC/BN/SiC oxidation was twice that measured for the MI SiC/BN/SiC composite. The increased composite degradation rates compared to the monolithic SiC can be attributed primarily to the presence of B-containing phases in the composite structure. There are multiple concurrent reactions during composite oxidation. In addition to the formation of SiO_2 due to SiC matrix and fiber oxidation, BN also oxidizes to form B_2O_3. Silica and boria then react to form borosilicate glass. Not only are the SiC and BN oxidation reactions accelerated in the presence of water vapor, but reactant diffusivities through the subsequently formed borosilicate glass are high, thereby further increasing the degradation rates of the composite constituents.[5] Impurities present in these commercial composites also increase the oxidation rates, particularly in the presence of water vapor.[9] Besides the accelerated oxidation, excessive amounts of gaseous reaction products are formed resulting in highly defective, non-protective, surface products (such as in the silica scale, refer to Figure 4).

Clearly, the amount of borosilicate that forms and its viscosity depends on the amount of BN (and additional B-containing phases) present in the starting material. The CVI SiC/BN/SiC contains significantly more boron than the MI SiC/BN/SiC. Therefore, higher degradation rates for this composite are expected and are observed (Figure 10). Greater amounts of borosilicate glass form and this increases the overall composite degradation rate. The formation of significant amounts of gaseous reaction products during oxidation is evident by the the formation of a highly defective borosilicate glass surface product (see bubble-like voids in Figure 7). Also, the starting CVI composite has >10 vol% interconnected, large scale porosity which allows these reactions to take place in areas well below the exposed surface of the composite. Pore surfaces are oxidized, and once the SiC is breached, extensive borosilicate glass forms and consumes the fiber tows. The MI SiC/BN/SiC is near full density and, thus, sub-surface oxidation does not occur.

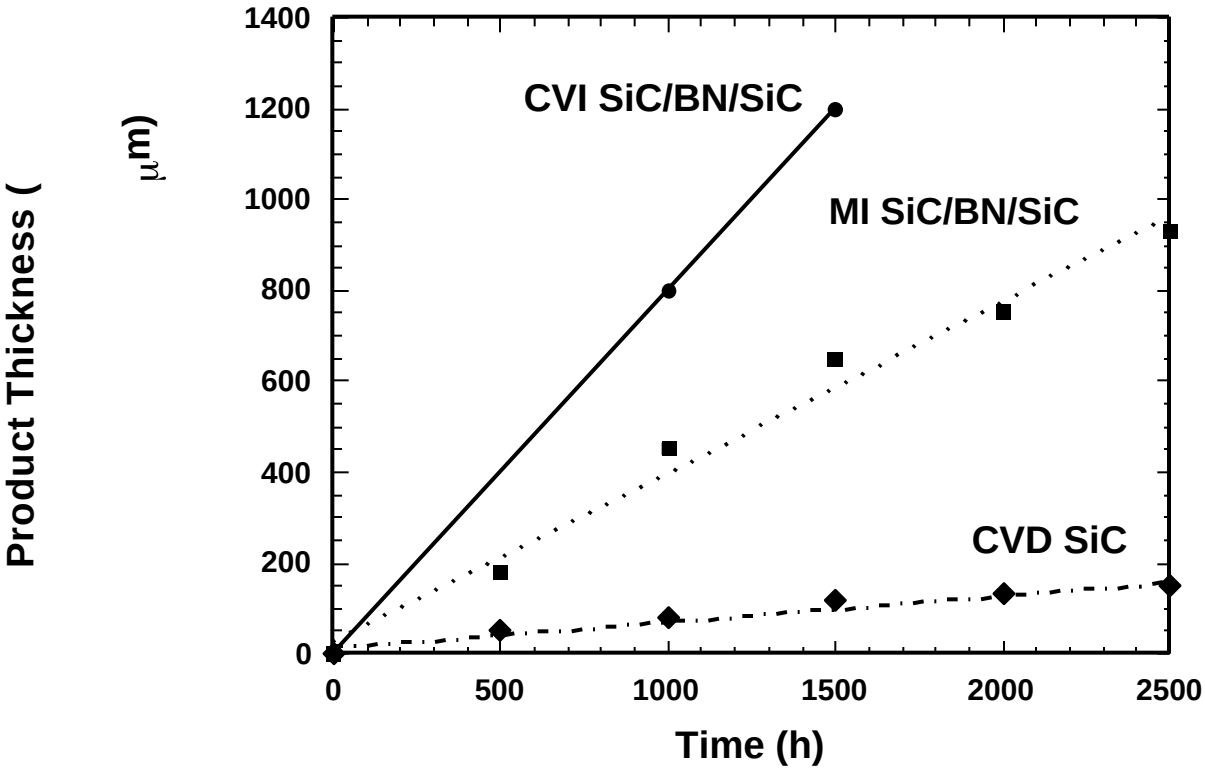

Figure 10. Comparison of the oxidation behaviour of MI and CVI SiC/SiC composite vs. monolithic SiC oxidation (product thickness vs. time). The CVI composite has a much greater concentration of boron-containing phases than the MI composite.

5. SUMMARY

The overall oxidation behavior of different composites at high water vapor pressures has been explained based on the concurrent surface reactions involving the formation of silica, boria, borosilicate glass, and gaseous reaction products. The higher degradation rate for the CVI SiC/BN/SiC composite is a result of (1) the increased amount of BN and B-containing phases in this composite and (2) the larger amount of interconnected, sub-surface porosity compared with the MI SiC/BN/SiC. The much faster degradation rates of both the MI and CVI composites compared to CVD SiC can be attributed to the presence of boron and the formation of borosilicate glass which significantly increases the oxidation rate of the primary composite constituent, SiC.

6. ACKNOWLEDGEMENTS

The authors wish to thank M. Howell and K.S. Trent for technical asssistance and J.R. Keiser and H.T. Lin for reviewing the manuscript. This research was sponsored by the U.S. Department of Energy, Assistant Secretary for Energy Efficiency and Renewable Energy, Office of Industrial Technologies, as part of the Continuous Fiber-Reinforced Ceramic Composite (CFCC) Program under contract DE-AC05-00OR22725 with UT-Battelle LLC.

7. REFERENCES

1. NASLAIN R., DUGNE O., GUETTE A., J. Amer. Ceramic Soc. **74**[1] (1991) pp. 2482-2488.
2. LOWDEN R.A., SCHWARZ O.J., MORE K.L., Ceramic Eng. Sci. Proc. **14**[7-8] (1993) pp. 375-384.
3. MORSCHER G.N., J. Amer. Ceramic Soc. **80**[8] (1997) pp. 2029-2042.
4. JACOBSON N.S., FARMER S., J. Amer. Ceramic Soc. **82**[2] (1999) pp. 393-398.
5. JACOBSON N.S., MORSCHER G.N., BRYANT D.R., TRESSLER R.E., J. Amer. Ceramic Soc. **82**[6] (1999) pp. 1473-1482.
6. MORE K.L., TORTORELLI P.F., LIN H.T., LARA-CURZIO E., LOWDEN, R.A., Proc. of The Electrochem. Soc., **98-9**, P.Y. Hou, et. al., Eds., The Electrochem. Soc., Pennington, NJ (1998) pp. 382-394.
7. DEAL B.E., GROVE A.S, J. Appl. Phys. **36**[12] (1965) pp. 3770-3778.
8. OPILA E.J., HANN R.E., J. Amer. Ceramic Soc. **80**[1] (1997) pp. 197-205.
9. OPILA E.J., J. Amer. Ceramic Soc. **82**[3] (1999) 625-636.
10. MORE K.L., TORTORELLI P.F., FERBER M.K., KEISER J.R., J. Amer. Ceramic Soc. **83**[1] (2000) 211-213.
11. MORE K.L., et. al., Proc. of TURBOEXPO ‘99, Paper #99-GT-292, ASME, New York, NY (1999).
12. MIRIYALA N., PRICE J.R., Proc. of ASME TURBOEXPO 2000, Paper #2000-GT-648, ASME, New York, NY (2000).
13. GRAY P., HEADINGER M., MILLER A., Ceramic Eng. Sci. Proc. **17** (1996) pp. 865-877.
14. LUTHRA K.L., SINGH R.N., BRUN M.K., Amer. Ceramic. Soc. Bull. **72**[7] (1993) pp. 79-85.
15. KEISER J.R., HOWELL M., WILLIAMS J.J., ROSENBERG R.A., Proc. Corrosion/96, Paper #140, NACE International, Houston, TX (1996).